Available online at www.sciencedirect.com
ScienceDirect
Journal of the European Ceramic Society 28 (2008) 701–710
www.elsevier.com/locate/jeurceramsoc

Green strength testing of pressed compacts: An analysis of the different methods

J.L. Amorós *, V. Cantavella, J.C. Jarque, C. Felíu

Instituto de Tecnología Cerámica, Asociación de Investigación de las Industrias Cerámicas, Universitat Jaume I. Castellón, Spain

Received 14 July 2007; received in revised form 13 September 2007; accepted 15 September 2007
Available online 7 November 2007

Abstract

This paper presents a comparative study of three- and four-point bending tests and diametral compression (DC) tests, used to measure the mechanical strength of green pressed compacts. The study has been conducted on pressed ceramic test pieces, formed at different pressing conditions. It was found that Weibull statistics largely explained the differences in the results of the three-point and four-point bending tests. However, Weibull statistics could not explain the much lower mechanical strength obtained with the diametral compression tests. The study establishes a correlation between the bending and DC tests; however, this correlation depends on moisture content, which is directly related to the plasticity of the piece. This finding confirms that the types of mechanical tests studied do not have the same sensitivity to the factors that lead to fracture. The differences in mechanical strength between the bending and DC tests were explained using a suitable fracture criterion (based on maximum strain) and plastic deformation.
© 2007 Elsevier Ltd. All rights reserved.

Keywords: Pressing; Green strength; Clays

1. Introduction

Dry pressing is an economical yet versatile technique for high volume production of ceramic parts with low to moderate geometrical complexity. Green mechanical strength is one of the most important properties of green pressed bodies, since it is essential these compacts should be able to withstand the thermal and mechanical stresses they undergo during the pre-firing stages without deterioration. In addition to green handling consideration, green strength can be indicative of how well a ceramic processing system is working.[1–3] Defects originating during the earliest stages of processing have been shown to persist into the final product.[4–6] The absence of appropriate green tile mechanical properties leads to product losses (in both unfired and fired tiles), with the ensuing costs involved in disposing of, or reintroducing the arising scrap in the production process, in addition to the associated environmental impact. Current product losses from cracking and breakage of green tiles are estimated at 3%, whereas fired product losses from cracks in green tiles are estimated at about 2%. This means that in Europe alone, every year, the product losses associated with cracks and breakages amount to around 200 million euros, in addition to some 6.25×10^8 kg of solid wastes that mainly go to landfills.

Historically, green strength has been evaluated using three- or four-point bending tests, and reported as modulus of rupture. These tests have been used to overcome the inherent difficulty of tensile testing of elastic materials: unwanted stresses from the gripping devices prevent accurate bulk measurements. A limitation of bend tests is that only the surface is subjected to maximum stress and failure is initiated by surface rather than bulk flaws. The diametral compression test, also called the indirect tensile test or Brazilian test, which was introduced around 1950 to measure the tensile strength of concrete[7–9], has gained popularity because of simplified piece preparation, simple geometry, and quickness of testing. Thus, it was very early implemented in many technological fields, such as rocks[10,11], ceramics[12–15], metal composites[16], materials used in dentistry[17–19], and materials used in the processing of pharmaceutical dosage forms.[20–24]

A significant distinction is to be noted, however, between the tensile fracture stress obtained from the bending tests and

* Corresponding author.
E-mail address: joseluis.amoros@itc.uji.es (J.L. Amorós).

0955-2219/$ – see front matter © 2007 Elsevier Ltd. All rights reserved.
doi:10.1016/j.jeurceramsoc.2007.09.040

that obtained from the diametral compression test: the former pertains to a strictly uniaxial stress state, while the latter is associated with a transverse compressive stress considerably greater than the tensile stress. As a result, the tensile fracture stress obtained from the bending test (the uniaxial stress condition) will be greater than that derived from the disk test (a biaxial stress condition). In addition, the ratio of bend strength to diametral compression strength depends (in a complex way) on the piece sizes used, and particularly on the nature of the material itself.[25,26] On the other hand, anomalous results may be obtained from this test when the material is relatively soft[20] or exhibits a limited plastic deformation before fracture.[21–23]

In the last three decades, diametral compression has become the most widely used test in the green strength testing of pressed ceramic compacts.[27–30] In the mechanical tests, however, these intermediate products can undergo appreciable macroscopic plastic deformation, depending on their characteristics,[31,32] possibly calling into question the applicability of the diametral compression test. However, a literature survey found no study in which the different tests for evaluating the mechanical strength of pressed green ceramic compacts were analysed and compared.

This paper presents a comparative analysis of the different methods proposed in the literature for the determination of the mechanical strength of pressed compacts, in terms of simplicity in interpreting the experimental results and accuracy of these results. In addition, it has been attempted to explain the differences found between the mechanical strength values obtained by the different tests.

2. Experimental procedure

To conduct the study a granulated industrial spray-dried pressing powder was used, with a stoneware floor tile-type of composition.[33] The composition consisted of a mixture of red illitic-kaolinitic clays with abundant quartz, to which a small quantity of sodium tripolyphosphate and sodium metasilicate was added as a suspension dispersant. The mean size of the spray-dried granules was about 400 μm.

The mechanical tests were performed on test pieces of differing compactness, ϕ, formed by pressing (at different pressures, P, and different agglomerate powder moisture contents, X_p). The test procedure followed is illustrated in the flow chart of Fig. 1. It shows the importance assigned to the value of test compact bulk density, as noted previously,[35,36] since this variable is indicative of the compact's internal microstructure.

An Instron model 4502 universal testing machine was used to perform the mechanical strength tests on the green ceramic bodies, loading at a rate of 1 mm/min. Three methods of measuring mechanical strength have been analysed: three-point bending (3B), Fig. 2a; four-point bending (4B), Fig. 2b; and diametral compression with direct load application (DC), Fig. 3a.

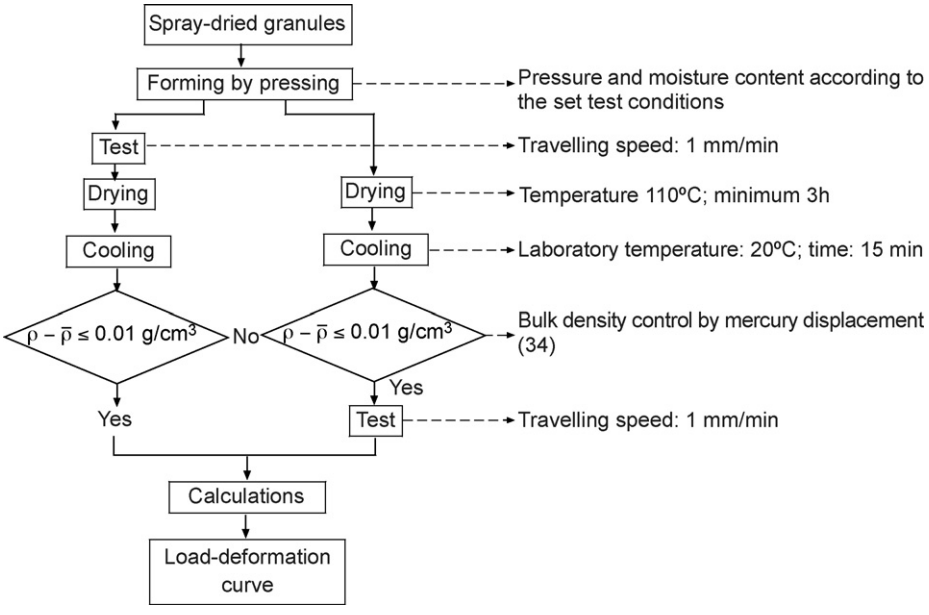

Fig. 1. Flow chart of the test procedure followed. See Ref. [34].

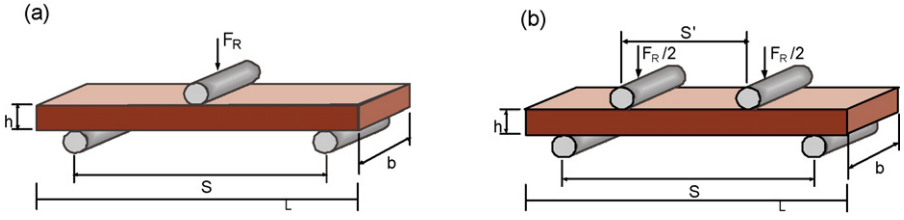

Fig. 2. Schematic illustration of the experimental 3B (a) and 4B (b) test set-up.

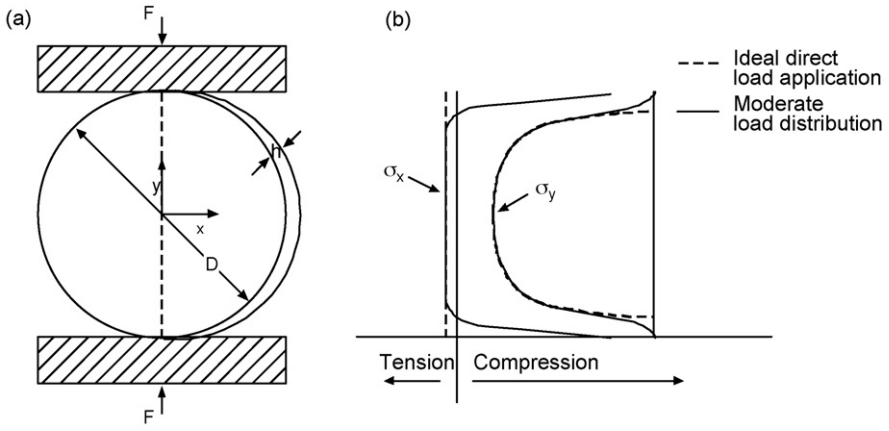

Fig. 3. Diametral compression test. (a) Experimental device with direct load application. (b) Stress distribution along the vertical diametral plane.

The bending tests were conducted with parallelepiped test pieces, L.b.h, set on two support rods separated by a distance S, applying the load, F, through one single top rod (3B) or through two top rods (4B) until fracture at $F = F_R$. Bending tests are very sensitive, however, to the surface characteristics of the bar face that is subjected to tensile stress (the face opposite the one onto which the load is applied) and, in addition, the two faces of the pressed piece usually display quite different surface characteristics, owing to the pressure gradient that develops in the axial direction during pressing. As a result, in order to determine the magnitude of both effects on the mechanical strength of the piece, two series of experiments were prepared, each with six test pieces, under the same pressing conditions; the bar face subjected to tensile stress in the three-point bending (3B) test was changed from one series to the other. It was found that when the face subjected to tensile stress was also the face onto which the pressing load had been applied, the strength values obtained were 8% higher than when the opposite circumstance occurred. In view of this, the most unfavourable situation was adopted as a criterion in all the bending tests conducted, i.e., subjecting the less pressed face to tensile stress.

In the diametral compression test, the test piece was a disk with diameter D and thickness h, and the load F, was applied at two diametrically opposite points until fracture at $F = F_R$. This ideal loading (Fig. 3a), produces a biaxial stress distribution within the elastic disk, which was calculated by Hertz in 1895,[22] illustrated in Fig. 3b. The Hertzian solution shows that along the loaded diameter, the normal stress, σ_x, is tensile and constant:

$$\sigma_x = \frac{2F}{\pi Dh} \quad (1)$$

σ_y, parallel to the loaded diameter, is a compressive stress. This increases from $3\sigma_x$ at the centre of the disk to infinity beneath the loading points. The shear stress is zero along the diameter plane and hence σ_x and σ_y are the principal stresses on the plane. In practice, the load needs to be distributed over a finite area to avoid shear and/or compression failure at the loading points.[26] The effects of load distribution are illustrated in Fig. 3b. The stress distribution near the centre is virtually unaffected by the change in load distribution over a moderate area (load area width 0.15 times the diameter of the disk).[37] Near the ends σ_x becomes compressive, while the previously high compressive values of σ_y are considerably reduced, and hence the possibility of disk fracture at the loading points. Thus, assuming that the maximum tensile principal stress, σ_x, is responsible for the failure, the tensile strength, σ_{DC}, (Table 1) is obtained by substituting F_R for F in Eq. (1).

Since these green compacts exhibit an appreciable plastic and elastic deformation prior to fracture, the applied load is distributed on a sufficiently large contact area for fracture to occur by tension in the diametrical plane of the disk, in principle without requiring the use of pads or other means of load distribution. When a thin graphite layer was applied onto the plates and the track was measured at the edge of the disk after the test had been conducted, it was verified that, even for the least deformable disks, the ratio: length of the load distribution arc/test piece diameter was larger than 0.15. Fracture by shear was not observed in any of the test pieces. In view of the foregoing, direct load application was used, as other researchers have done, to determine the mechanical strength of the green pieces.[29–30]

Given the scatter found in the experimental breaking load values under the same test conditions (owing to the impossibility of fixing, in an absolutely rigorous and accurate way, the internal microstructure of the test pieces and hence the presence of imperfections such as pores of varying size, small microcracks, etc.), it was attempted to apply different statistical theories for the experimental data treatment. The most widely used theory at present is Weibull statistics, which was ultimately chosen.

The strength data, σ ($\sigma = \sigma_{DC}, \sigma_{3B}, \sigma_{4B}$, calculated from the equations in Table 1), have been analysed with the usual two-parameter empirical formula relating the probability of failure,

Table 1
Equations used for the determination of mechanical strength. The meaning of the geometric parameters is shown in Figs. 2 and 3

Method	Equation
Three-point bending (3B)	$\sigma_{3B} = \frac{3}{2}\frac{S}{bh^2}F_R$
Four-point bending (4B)	$\sigma_{4B} = \frac{3}{2}\frac{S-S'}{bh^2}F_R$
Diametral compression (DC)	$\sigma_{DC} = \frac{2}{\pi}\frac{1}{Dh}F_R$

F_R is the load applied at fracture.

Table 2
Characteristic dimensions of the test pieces and assemblies used in the tests for determining mechanical strength

Method	L (mm)	D (mm)	S (mm)	S' (mm)	b (mm)	h (mm)
3B	80	–	60	–	20	7
4B	80	–	60	30	20	7
DC	–	40	–	–	–	7

p_f, to fracture strength, σ,

$$p_f = 1 - \exp\left[-\left(\frac{\sigma}{\sigma_0}\right)^m\right] \quad (2)$$

where m (Weibull modulus) is a parameter that allows the scatter of the experimental mechanical strength data to be characterised, and σ_0 is a normalising factor. The strength data, σ, are ranked in order and assigned a probability of failure, p_f, according to the formula $p_f = i/(N+1)$, where 'i' is the ith piece. The Weibull modulus, m, is the slope of a plot of $\ln[\ln(1/(1-p_f))]$ vs. $\ln(\sigma)$.

To apply Weibull statistics, 25 pieces were prepared for each operating condition. The pieces that failed to meet the constraint imposed on the bulk density value (Fig. 1) were discarded. More than 20 pieces were tested in every case.

Table 2 details the dimensions of the test pieces and of the assemblies used to conduct the different mechanical rupture tests illustrated in Figs. 2 and 3.

3. Results and discussion

3.1. Dry and as-pressed mechanical strength of test pieces formed at different pressures and different agglomerate powder moisture contents, X_p. Comparison between different tests

Disks and bars were formed under usual industrial pressing conditions, $P = 30$ MPa and $X_p = 0.05$ kg water/kg dry solid, and under four other, extreme conditions that yielded very different compactnesses, ϕ and, hence, very different microstructures and mechanical behaviours from those found in industrial practice.

The three types of mechanical tests were conducted on as-pressed and dry test pieces. The mechanical strength values were treated by Weibull statistics. In order to compare the results with those reported in the literature, the coefficients of variation, CV, of the measurements, as well as the ratio between the standard deviation and the mean value of the measurements, $\bar{\sigma}$, expressed as a percentage, were also determined.

Table 3 details the results of the mechanical tests, together with the values of the pressing variables, P and X_p, used and the resulting compactnesses (ϕ).

In general it was verified that the individual mechanical strength values, σ, for each series of test pieces fitted the Weibull statistics quite well, since the plot of the values $\ln\ln(1/p_s)$ vs. $\ln\sigma$ yielded straight lines (Fig. 4), with correlation coefficients above 0.9 in all cases, and above 0.95 in most.

In addition, the measurement scatter was generally small, even though appreciable differences existed between the coefficients of variation (CV) for each set of measurements. Thus, the CV was <6% in all cases, except those corresponding to the four-point bending (4B) tests of the as-pressed test pieces, σ^P_{4B}, which yielded high values (about 7% <CV < 10%). Analogously, the Weibull moduli (m) were generally higher than 20; only the values corresponding to the series of test pieces indicated previously, σ^P_{4B}, were considerably lower ($10 < m < 15$). In any event, the values obtained for CV and m were, as a whole, of the same order as those reported in the literature.[26–28]

On the other hand, it was verified that, independently of the type of test used, the mean mechanical strength values of both the dry test pieces ($\bar{\sigma}^d$) and the as-pressed test pieces ($\bar{\sigma}^p$) increased considerably with compactness (ϕ) and that, at the same ϕ, the dry test pieces were substantially stronger than the as-pressed test pieces.[32,39,40]

3.1.1. Comparison between three-point bending (3B) and four-point bending (4B) tests

When the results corresponding to the 3B and 4B tests are compared, the mean mechanical strength values of the dry test pieces, $\bar{\sigma}^d_{3B}$, and the as-pressed test pieces, $\bar{\sigma}^p_{3B}$, are observed to be slightly higher than those obtained by the 4B tests, $\bar{\sigma}^d_{4B}$, and, $\bar{\sigma}^p_{4B}$. These outcomes are consistent with the Weibull theory and with a high value of m. In effect, in addition to quantifying the scatter of the mechanical strength values for a series of test pieces hypothetically having the same characteristics, Weibull statistics allows the mean values of this property, measured by different tests, to be related based on the concept of the effective volume, which in turn depends on the volume of the test piece subjected to loading and on the type of load applied in each test.[41,42] In the case at hand, the equation that describes the ratio between the mean mechanical strength values obtained in the respective tests is as follows:

$$\frac{\bar{\sigma}_{4B}}{\bar{\sigma}_{3B}} = \left(\frac{2}{m+2}\right)^{1/m} \quad (3)$$

According to this expression, at a high value of m (exceeding 25 in most of the studied series), the values of $\bar{\sigma}_{4B}$ will be slightly lower than those of $\bar{\sigma}_{3B}$ (in this case $\bar{\sigma}_{4B} < 0.9\bar{\sigma}_{3B}$).

It should also be noted that the scatter in the measurements obtained by the 3B tests is smaller than that of the corresponding measurements obtained by the 4B tests, as may be observed when the respective values of the Weibull modulus, m, and of the coefficient of variation, CV, are compared. These results clearly show that the values of the measurement scatter and of the Weibull modulus do not depend exclusively on the microstructural characteristics of the material, but that other experimental factors, originating in the mechanical test itself and/or in the test piece preparation procedure, may also affect the values of these parameters, at times even quite significantly. Thus, the existence has been experimentally verified of small compactness, ϕ, and thickness gradients along the length of the bar, generally related to non-uniform distribution of the pressing powder during die filling and/or differences in punch alignment during the pressing operation. These variations will be more critical in the 4B test than in the 3B test, since in the 4B test the maximum stress covers the entire surface of the bar face between the two internal

Table 3
Mean dry ($\bar{\sigma}^{d}$) and as-pressed ($\bar{\sigma}^{p}$) mechanical strength, Weibull moduli (m), coefficients of variation (CV) and regression coefficient of the fits (R^2) obtained in the different tests with dry and as-pressed test pieces

P (MPa)	X_p (kg water/kg dry solid)	ϕ	$\bar{\sigma}^{d}_{3B}$ (MPa)	CV (%)	m	R^2	$\bar{\sigma}^{p}_{3B}$ (MPa)	CV (%)	m	R^2
Three-point bending (3B)										
15	0.03	0.665	1.10	2.9	42	0.97	0.42	5.8	19	0.96
	0.07	0.718	3.10	3.5	35	0.97				
30	0.05	0.750	3.33	3.4	30	0.95	1.38	4.9	22	0.95
60	0.03	0.754	3.37	3.3	32	0.93				
	0.07	0.802	6.55	4.2	29	0.96	2.40	4.7	23	0.97
Four-point bending (4B)										
15	0.03	0.665	0.97	5.7	20	0.96	0.35	9.4	11	0.97
	0.07	0.718	2.97	4.2	28	0.90				
30	0.05	0.750	3.18	4.5	22	0.91	1.30	8.1	13	0.96
60	0.03	0.754	3.25	5.5	18	0.90				
	0.07	0.802	6.37	4.4	25	0.97	2.35	7.5	15	0.95
Diametral compression (DC)										
15	0.03	0.665	0.50	4.3	27	0.94	0.22	3.5	34	0.95
	0.07	0.718	1.51	3.0	38	0.90				
30	0.05	0.750	1.53	3.5	32	0.93	0.47	3.5	36	0.94
60	0.03	0.754	1.57	4.0	29	0.93				
	0.07	0.802	2.79	4.0	27	0.97	1.01	2.1	40	0.90

supports, in contrast to the 3B test in which this stress is only located at the centre segment of this face.

Similarly, certain deficiencies or errors associated with bend tests, such as the unequal distribution of moments, twisting or wedging, occur more frequently and their effect is much more critical in the 4B than in the 3B test.[43]

The values of the ratios $\bar{\sigma}^{d}_{3B}/\bar{\sigma}^{d}_{4B}$ and $\bar{\sigma}^{p}_{3B}/\bar{\sigma}^{p}_{4B}$ of the dry and as-pressed bars have been plotted versus the corresponding compactness values, ϕ, in Fig. 5. The figure shows that the mean values of both ratios decrease as test piece compactness increases, tending asymptotically to a value close to 1, at ϕ = 0.8, the maximum compactness reached in this study. The values of both ratios, $\bar{\sigma}^{d}_{3B}/\bar{\sigma}^{d}_{4B}$ and $\bar{\sigma}^{p}_{3B}/\bar{\sigma}^{p}_{4B}$, and of Eq. (3) were used to calculate the new values of the Weibull modulus, m_c. These values, calculated in the form $1/m_c$, have been plotted versus those of compactness, ϕ, in Fig. 6. The figure shows that as compactness, ϕ, increases, the values of $1/m_c$ decrease, tending asymptotically to a very small value (very large m_c), at values of ϕ = 0.8. Unlike the values of m, detailed in Table 3, obtained by fitting the individual mechanical strength values to Eq. (2), which depended on the type of test and did not display a logi-

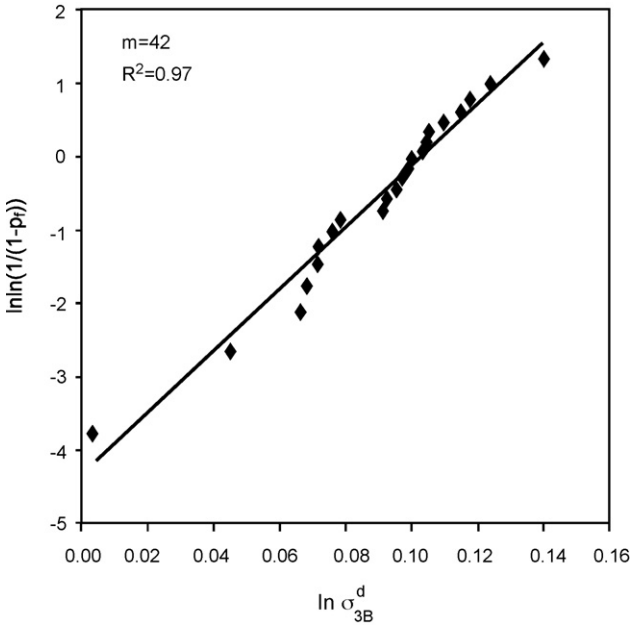

Fig. 4. Weibull plot of results obtained by the three-point bending test for test specimens formed at P = 15 MPa and X_p = 0.03 kg water/kg dry solid.

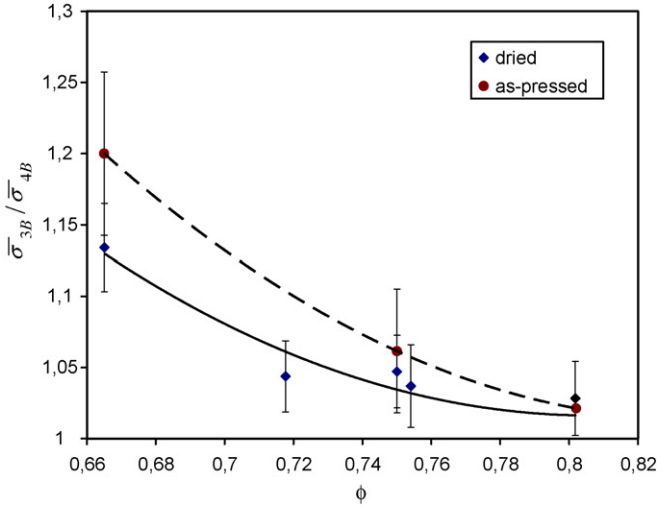

Fig. 5. Evolution of the ratio of three-point bend strength to four-point bend strength for as-pressed, $\bar{\sigma}^{P}_{3B}/\bar{\sigma}^{P}_{4B}$, and dried, $\bar{\sigma}^{d}_{3B}/\bar{\sigma}^{d}_{4B}$, test pieces with compactness, ϕ.

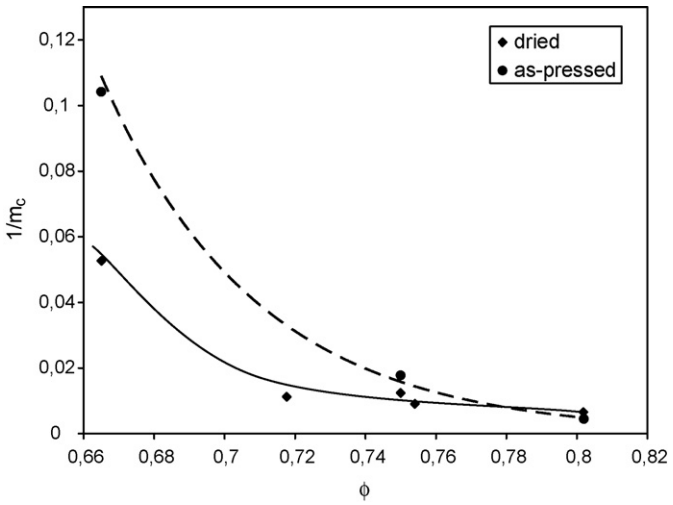

Fig. 6. Evolution of $1/m_c$ with compactness, ϕ, for as-pressed and dried pieces.

cal variation with piece compactness, ϕ, the new values of the Weibull modulus, m_c, calculated from Eq. (2), only depend on the characteristics of the material and follow a logical trend. Indeed, in accordance with the Weibull theory, m_c increases ($1/m_c$ decreases) as piece compactness, ϕ, increases, piece compactness being directly related to the material's microstructural homogeneity. Thus, as pressing pressure, P, and/or the moisture content of the agglomerate, X_p, rises, piece compactness, ϕ, increases and with it, microstructural homogeneity, mainly owing to the progressive elimination of intergranular pores, granule deformation, and granule compaction.[32,44,45] These transformations are also displayed in a similar way by a progressive reduction of surface heterogeneities in the piece, ultimately responsible for the material's flexural strength.

3.1.2. Comparison between diametral compression and bending tests

The results in Table 3 show that the mean mechanical strength values obtained by diametral compression of both the dry disks, $\bar{\sigma}^{d}_{DC}$, and the as-pressed disks, $\bar{\sigma}^{p}_{DC}$, are much lower than those obtained in the bend tests of both the dry bars, $\bar{\sigma}^{d}_{3B}$ and $\bar{\sigma}^{d}_{4B}$, and the as-pressed bars, $\bar{\sigma}^{p}_{3B}$ and $\bar{\sigma}^{p}_{4B}$. Furthermore, when the results of the dry piece tests are compared, the measurement scatter in the diametral compression tests, $\bar{\sigma}^{d}_{DC}$, ($3\% < CV < 4.5\%$) is comparable to that found in the 3B tests, $\bar{\sigma}^{d}_{3B}$, ($3.5\% < CV < 4.5\%$), while it is smaller than that in the 4B tests, $\bar{\sigma}^{d}_{4B}$, ($4\% < CV < 6\%$). However, when the results of the as-pressed, and hence wetter, pieces are analysed, the measurement scatter in the diametral compression tests, $\bar{\sigma}^{p}_{DC}$, ($2\% < CV < 3.5\%$) is lower than that in the 3B tests, $\bar{\sigma}^{p}_{3B}$, ($5\% < CV < 6\%$), and considerably lower than that in the 4B tests, $\bar{\sigma}^{p}_{4B}$, ($7.5\% < CV < 9.5\%$). In addition, the decrease in plasticity or ductility of the test pieces (from as-pressed to dry pieces) led to a rise in measurement scatter in the bending tests, while the opposite occurred in the diametral compression tests. This behaviour is assignable to the pronounced effect that a material's plasticity has on its mechanical response during the test, this being much greater in the diametral compression test than in the bending test. Thus, the as-pressed disks undergo greater deformation, principally of a plastic nature, at the edges of the disk in contact with the plate, than the dry disks. This leads to a greater load distribution, and to a reduction in the adverse effects stemming from poor disk alignment between the plates or from the presence of geometrical irregularities at the edges of the disk. The graphite marking test showed, in fact, that the ratio: length of the load distribution arc/test piece diameter increased considerably with the material's moisture content, X, going from a value of 0.15 ± 0.02 for dry test pieces, $X = 0.00$ kg water/kg dry solid, to a value of 0.20 ± 0.02 for as-pressed disks at $X = X_p = 0.05$ kg water/kg dry solid, even reaching 0.25 ± 0.02 for values of $X = X_p = 0.07$ kg water/kg dry solid. Either factor, or a combination of both, will probably contribute to reducing the measurement scatter obtained in the diametral compression, DC, of wet test pieces.

In regard to the Weibull modulus, m, this behaves as might be expected, if it is taken into account that the increased measurement scatter (higher CV) involves a decrease in m.

The mechanical strength values of the as-pressed bars, σ^{p}_{3B}, and dry bars, σ^{d}_{3B}, obtained in the 3B tests have been plotted versus the corresponding diametral compression data, σ^{p}_{DC} and σ^{d}_{DC}, in Fig. 7. The plots obtained after treatment of the results from the 4B tests, σ^{p}_{4B} and σ^{d}_{4B}, and from the diametral compression tests, σ^{p}_{DC} and σ^{d}_{DC}, are quite similar and have therefore been omitted.

It may be observed that the results corresponding to the dry test pieces fit quite well a straight line that passes through the origin, indicating that the ratio $\bar{\sigma}^{d}_{3B}/\bar{\sigma}^{d}_{DC} = 2.20$ is practically independent of the operating variables used in forming and, therefore, of the materials' microstructural characteristics. In contrast, the results corresponding to the as-pressed test pieces depart notably from the foregoing linearity, and better fit another straight line of greater slope, $\bar{\sigma}^{p}_{3B}/\bar{\sigma}^{p}_{DC} = 2.5$ These results suggest that the ratio $\bar{\sigma}_{3B}/\bar{\sigma}_{DC}$ is influenced by the elasto-plastic nature of the materials, just as occurred with the measurement scatter values. Thus, for dry materials, with a small plastic or

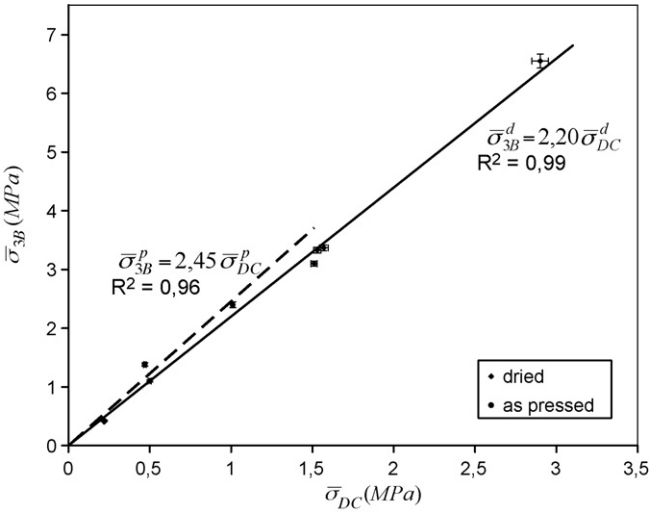

Fig. 7. Relation between three-point bend strength, $\bar{\sigma}_{3B}$, and diametral compression strength, $\bar{\sigma}_{DC}$, for as-pressed and dried pieces.

permanent deformation, the ratio $\bar{\sigma}^{d}_{3B}/\bar{\sigma}^{d}_{DC}$ is smaller than that corresponding to the as-pressed test pieces, $\bar{\sigma}^{p}_{3B}/\bar{\sigma}^{p}_{DC}$, which have a larger plastic deformation.

3.2. Analysis of the discrepancy between the mechanical strength values obtained in the bending and in the diametral compression tests

It has generally been observed in the literature that the strength values obtained in diametral compression testing, DC, are always much lower than for other uniaxial tests, such as three-point bending, 3B, and four-point bending, 4B. This discrepancy has been noted in materials that display clearly elastic behaviour, such as rocks,[26] plaster of Paris,[25] ceramics,[12–15] concrete,[8,9] as well as in elasto-plastic materials, metal matrix composites,[16] tablets,[20,21] etc.

Many reasons have been suggested to explain this discrepancy:

(i) The piece size effect, though not of itself explaining, in principle, the high $\bar{\sigma}_{3B}/\bar{\sigma}_{DC}$ ratio obtained, is a factor that may to some extent decrease the value of the ratio. Thus, in accordance with the Weibull theory, the ratio between the mean mechanical strength values $(\bar{\sigma}_{3B}/\bar{\sigma}_{DC})_{w}$ and the ratio of the effective volumes of the pieces in diametral compression, V_{DC}, and three-point bending, V_{3B}, is:

$$\left(\frac{\bar{\sigma}_{3B}}{\bar{\sigma}_{DC}}\right)_{W} = \left(\frac{V_{DC}}{V_{3B}}\right)^{1/m} \quad (4)$$

The effective volume of the pieces in three-point bending, V_{3B}, was calculated from the dimensions of the bar (Table 2), setting a value of $m = 20$ for the Weibull modulus and using the appropriate equation.[42] This yielded $V_{3B} = 58\,mm^3$. The same procedure was followed, using the appropriate equation,[46] to calculate the effective volume of the pieces in diametral compression, which yielded $V_{DC} = 556\,mm^3$. Substituting these values into Eq. (4) gives $(\bar{\sigma}_{3B}/\bar{\sigma}_{DC})_{W} = 1.12$. In this case, the 'volume effect' is found to be moderate, because despite the great difference in effective volume of the pieces, $V_{DC} \gg V_{3B}$, the value of the Weibull modulus is also high, $m \geq 20$.

(ii) It has also been suggested,[12,26] that fracture in brittle materials occurs when the maximum tensile strain reaches a critical value (maximum tensile strain criterion), rather than the maximum tensile stress (maximum tensile stress criterion). In the case of bending tests, both criteria are equivalent, since there is only tensile stress at the point of the fracture. However, in the diametral disk test (Fig. 3b), the centre of the disk is subjected to a compressive stress, σ_y, perpendicular to the tensile stress, σ_x, and the strains produced by the two stresses are in the same direction. As a result, the disk breaking stress must be multiplied by a factor of $(1 + 3\nu)$, where ν is Poisson's ratio, to convert the combined tensile and compressive stress at the centre of the disk to the effective uniaxial stress in accordance with the maximum strain criterion. If plastic flow occurs before brittle fracture, then ν will be 0.5 instead of a lower value to be expected in the elastic region ($\nu = 0.20$–0.30). Therefore, in accordance with the maximum tensile strain criterion, the ratio between bending strength, $\bar{\sigma}_{3B}$, and diametral compression strength, $\bar{\sigma}_{DC}$, will be:

$$\left(\frac{\bar{\sigma}_{3B}}{\bar{\sigma}_{DC}}\right)_{SC} = (1 + 3\upsilon) = 1.6 - 2.5 \quad (5)$$

depending on whether the behaviour of the material prior to fracture is plastic $(\bar{\sigma}_{3B}/\bar{\sigma}_{DC})_{SC} = 2.5$, or elastic $(\bar{\sigma}_{3B}/\bar{\sigma}_{DC})_{SC} = 1.6$. This fracture criterion, suggested by various researchers,[12,26] thus seems to provide a good explanation for the discrepancy, particularly if the material becomes plastic prior to fracture, as occurs in the present case, which is set out below.

(iii) Some researchers,[18,26,37] believe that failure may be attributed not only to the development of a tensile crack centre, but also to higher shear and compressive stresses which may be generated peripherically at the borderline of the loaded area. In the present case, since the widths of the loaded area are quite large (point 3.1.2) this is not very likely to be the cause of the discrepancy. A theoretical and numerical study[37] found that loaded area widths similar to those in this study assure, at least theoretically, crack initiation at the centre of the disk. In the present study, all pieces exhibited normal tensile fracture. No piece displayed compression or shear failure at the loading points.

(iv) Another possible cause of this discrepancy stems from the fact that during the diametral compression test most real materials do not display linear elastic behaviour, one of the basic requirements of the Hertzian solution (Fig. 3b), which is why the stress distribution in the diametrical plane of the disk and, in particular, the tensile stress, σ_x, responsible for the fracture may depart significantly from the theoretical value (Eq. (1)) used to calculate σ_{DC} (Table 1). In materials as brittle as tungsten carbide[14] it has been verified that whereas this material can remain elastic to the point of fracture in a bending test, it undergoes appreciable plastic flow before fracture in a disk test. This was suggested to be largely responsible for the fact that the maximum tensile stress at fracture is appreciably less in the disk test than in the bending test $(\bar{\sigma}_{DC}/\bar{\sigma}_{B} = 0.5)$. The load–deformation curves corresponding to the bending test of the dry bars and to the diametral compression test of the dry disks, both formed at $P = 30$ MPa and $X_p = 0.05$ kg water/kg dry solid, have been plotted in Fig. 8. It may be observed that in both curves, after a slight initial concave curvature associated with crushing at the contact points and/or elastic deformation of the measurement system,[32,37] a straight stretch follows, characteristic of the material's linear elastic response. In both cases, the departure from linearity (caused by crack propagation,[31,32] and/or plastic flow of the material[22,23] which defines the yield stress, σ_{yield}, always occurs before fracture of the test piece, σ_{DC} and σ_{3B}. However, comparison of these curves clearly shows that the straight stretch is shorter in the diametral compression test

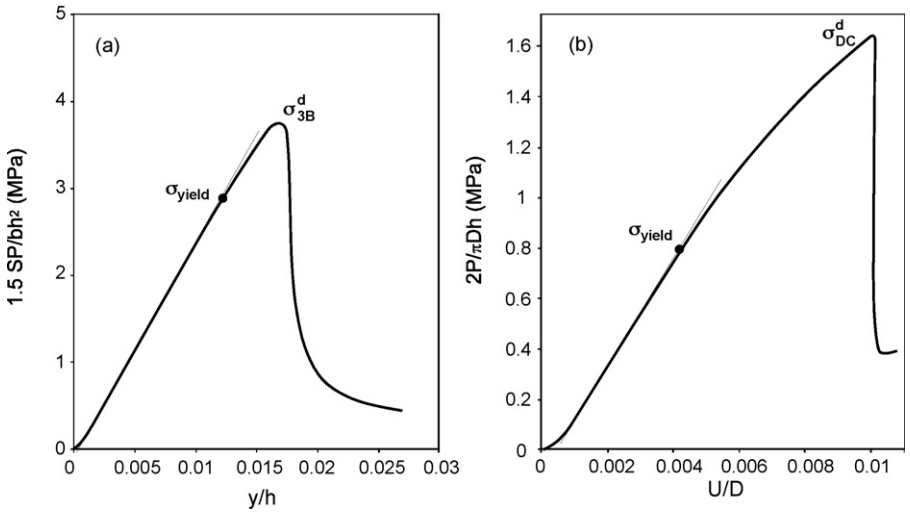

Fig. 8. Stress–strain curve, obtained by the three-point bending test (a) and by diametral compression (b), for dried specimens formed at $P = 30$ MPa and $X_p = 0.05$ kg water/kg dry solid.

than in the bending test. The same occurs with the ratio of the yield stress, σ_{yield}/rupture stress, σ_{DC} and σ_{3B}, for both tests. These results are consistent with the literature, since they show that the plastic response of the material, in the diametral compression test, DC, begins to appear much sooner than in the three-point bending test, even for the drier disks, which are the most brittle. In addition, in the diametral compression test, DC, the material yields at much lower stresses, σ_{yield}, than the rupture stresses, σ_{DC}.

In the case of plastically deforming materials, finite element simulations have confirmed a significant change in the maximum principal stress field (magnitude and location), rendering the equation for estimating tensile strength, σ_{DC}, (Table 1) invalid.[22] A map to verify the validity of this Hertzian equation has been proposed.[22] The ratio of the material's elastic to plastic properties, σ_{yield}/E, and the diametral strain at fracture in diametral compression, $(U/D)_R$, define this map. In view of this, based on the bending tests of the dry bars, $X = 0.00$ kg water/kg dry solid, formed under typical industrial pressing conditions ($P = 30$ MPa and $X_p = 0.05$ kg water/kg dry solid), the elastic modulus, E, and yield stress, σ_Y, have been calculated. This last property has been determined as the value of the stress at which a departure of 1% occurs in the linearity of the load–deformation curve. The values obtained were: $\sigma_Y/E = 0.85 \times 10^{-3}$ and $(U/D)_R = 10^{-2}$. These values lie in the Invalid Hertz Conditions region of the map (Fig. 9) since, for these plastically deforming materials, a maximum tensile stress of up to 2–3 times the elastic solution (Eq. (1)), located away from the compact centre, was obtained by simulation. As a result, these tensile stresses will lead to the initial formation of microcracks outside the centre of the disk at a much smaller load, F, than the load required to cause rupture in the centre of the disk in accordance with the elastic solution, F_R (Table 1). Therefore, this seems to be one of the causes that best explain the high $\bar{\sigma}_{3B}/\bar{\sigma}_{DC}$ ratio obtained experimentally in this study.

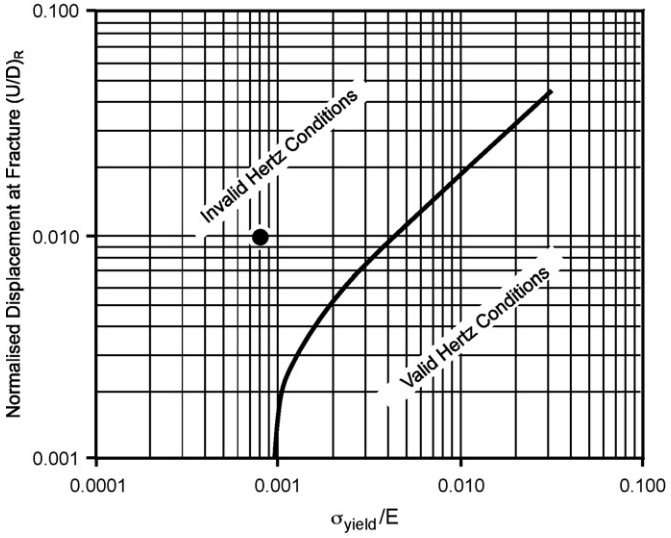

Fig. 9. Map proposed [21] to verify the validity of the Hertzian equation (Eq. (1)). The solid point represents the property ratio, σ_{yield}/E, and failure strain, $(U/D)_R$, of dried specimens formed at $P = 30$ MPa and $X_p = 0.05$ kg water/kg dry solid.

4. Conclusions

- The mean mechanical strength values obtained in this study by the three-point bending (3B) tests were slightly higher than those obtained by the four-point bending tests (4B). This result can be only partly explained by Weibull statistics, so that some other factors, such as compactness gradients or thickness variations in the piece may play an important role.
- The ratio between mechanical strength of the 3B and 4B tests, in as-pressed and dry test pieces, decreased when compactness increased. This is equivalent to a reduction of the inverse of the Weibull modulus ($1/m$), and is due to a more homogeneous microstructure (lower crack size scatter) of the pieces.

- Although there was a correlation between mechanical strength in bending and diametral compression, mechanical strength was much lower in diametral compression (DC) than in the bending tests (3B or 4B). This finding cannot be explained by differences in effective volume between bending and DC, derived from the Weibull statistics. The difference in mechanical strength can be explained by using the maximum strain fracture criterion (instead of the maximum stress) and the presence of some plastic deformation, though some other factors such as the shear stress near the contact may be non-negligible.
- The standard deviation of the dry test pieces was similar in the DC and 3B tests. When the as-pressed pieces were tested, however, the scatter was lower with diametral compression. The decreased scatter in the as-pressed DC pieces is likely to be associated with a higher plastic deformation.
- The stress–strain curves in the bending and DC tests confirmed that plastic deformation was larger in diametral compression. This finding is consistent with a map proposed in the literature to define the area of valid Hertz conditions, which indicates that, for the test pieces and experimental conditions used, the assumption of elastic behaviour is not met.

References

1. Carneim, T. J. and Green, D. J., Mechanical properties of dry-pressed alumina green bodies. *J. Am. Ceram. Soc.*, 2001, **84**(7), 1405–1410.
2. Kendall, K., Influence of powder structure on processing and properties of advanced ceramics. *Powder Technol.*, 1989, **58**, 151–161.
3. Hsieh, H. and Fang, T., Effect of green states on sintering behavior and microstructural evolution of high-purity barium titanate. *J. Am. Ceram. Soc.*, 1990, **73**(6), 1566–1573.
4. Shinohara, N., Okumiya, M., Hotta, T., Nakahira, K., Naito, M. and Uematsu, K., Formation mechanisms of processing defects and their relevance to the strength in alumina ceramics made by powder compaction process. *J. Mater. Sci.*, 1999, **34**, 4271–4277.
5. Zheng, J. and Reed, J. S., Effect of particle packing characteristics on solid state sintering. *J. Am. Ceram. Soc.*, 1989, **72**(5), 810–817.
6. Kendall, K., Alford, N. McN. and Birchall, J. D., The strength of green bodies. *Brit. Ceram. Proc.*, 1986, **8**, 255–265.
7. Carneiro, F. L. L. B. and Barcellos, A., Tensile strength of concretes. *Bulletin RILEM*, 1953, **13**, 97–107.
8. Akazawa, T., Methode pour l'essai de traction des betons. *Bulletin RILEM*, 1953, **16**, 12–23.
9. Wright, P. J. F., Comments on an indirect tensile test on concrete cylinders. *Mag. Concrete Res.*, 1955, 87–96.
10. Nova, R. and Zaninetti, A., An investigation into the tensile behavior of a schistose rock. *Int. J. Rock Mech. Min. Sci. Geomech. Abstr.*, 1990, **27**, 231–242.
11. Chen, C. S., Pan, E. and Amadei, B., Determination of deformability and tensile strength of anisotropic rock using Brazilian tests. *Int. J. Rock Mech. Min. Sci. Geomech. Abstr.*, 1998, **35**, 43–61.
12. Shaw, M. C., Braiden, P. M. and DeSalvo, G. J., The disc test for brittle materials. *Trans. ASME*, 1975, **96**, 77.
13. Marion, H. and Johnstone, J., A Parametric study of the diametral compression test for ceramics. *Ceram. Bull.*, 1977, **56**(11), 998–1002.
14. Takagi, J. and Shaw, M. C., Evaluation of fracture strength of brittle tools. *Ann. CIRP*, 1981, **30**(1), 53–57.
15. Ovri, J. E. O. and Davies, T. J., Diametral compression of silicon nitride. *Mater. Sci. Eng.*, 1987, **96**, 109–116.
16. Bonollo, F., Molinas, B., Tangerini, I. and Zambon, A., Diametral compression testing of metal matrix composites. *Mater. Sci. Technol.*, 1994, **10**(6), 558–564.
17. Ehrnford, L., Stress distribution in diametral compression tests. *Acta Odomol. Scand.*, 1981, **39**, 55–60.
18. Ehrnford, L., A fracture study of the diametral compression test by means of high-speed photography. *Acta Odontol. Scand.*, 1981, **39**, 71–77.
19. Ehrnford, L., The connection between load distribution and fracture load in the diametral compression test. *Exp. Study Sweden Dent. J.*, 1980, **4**, 201–212.
20. Stanley, P., Mechanical strength testing of compacted powders. *Int. J. Pharm.*, 2001, **227**, 27–38.
21. Amin, M. C. I. and Fell, J. T., Tensile strength and bonding in compacts: a comparison of diametral compression and three-point bending for plastically deforming materials. *C.I Amin. Drug Develop. Ind. Pharm.*, 2002, **28**(7), 809–813.
22. Procopio, A. T., Zavaliangos, A. and Cunningham, J. C., Analysis of the diametrical compression test and the applicability to plastically deforming materials. *J. Mater. Sci.*, 2003, **38**, 3629–3639.
23. Wynnyckyj, J. K., The correlation between the strength factor and the true tensile strength of agglomerate spheres. *Can. J. Chem. Eng.*, 1985, **63**(8), 591–597.
24. Galen, S. and Zavaliangos, A., Strength anisotropy in cold compacted ductile and brittle powders. *Acta Mater.*, 2005, **53**, 4801–4815.
25. Rudnick, A., Hunter, A. R. and Holden, F. C., An analysis of the diametral-compression test. *Mater. Res. Stand.*, 1964, **4**(5), 218–220.
26. Darvell, B. W., Uniaxial compression tests and the validity of indirect tensile strength. *J. Mater. Sci.*, 1990, **25**, 757–780.
27. Brewer, J. A., Moore, R. H. and Reed, J. S., Effect of relative humidity on the compaction of barium titanate and manganese zinc ferrite agglomerates containing polyvinyl alcohol. *Ceram. Bull.*, 1981, **60**(2), 212–216.
28. Walker, W. J. and Reed, J. S., Green testing of pressed compacts. *Ceram. Eng. Sci. Proc.*, 1993, **14**(11–12), 43–57.
29. Baklouti, S., Chartier, T. and Baumard, J. F., Mechanical properties of dry-pressed ceramic green products: the effect of the binder. *J. Am. Ceram. Soc.*, 1997, **80**(8), 1992–1996.
30. Uppalapati, M. and Green, D. J., Effect of external lubricant on mechanical properties of dry-pressed green bodies. *J. Am. Ceram. Soc.*, 2005, **88**(6), 1397–1402.
31. Lam, D. C. C. and Kusakari, K., Microstructure and mechanical properties relations for green bodies compacted from spray dried granules. *J. Mater. Sci.*, 1995, **30**, 5495–5501.
32. Amorós, J. L., Felíu, C. and Agramunt, J. V., Mechanical strength and microstructure of green ceramic bodies. *Cer. Acta*, 1996, **8**(6), 5–19.
33. Amorós, J. L., García, J., Sánchez, E. and García, M. C., Composiciones para la Fabricación de Baldosas Cerámicas. Influencia de los Distintos Componentes sobre su Comportamiento en el Proceso de Fabricación. *Cerámica Información*, 1998, **243**, 37–43.
34. Amorós, J. L., Blasco, A., Manfredini, T. and Pozzi, P., A new experimental method for measuring apparent density in ceramics: aspects of technique and applications. *Ind. Ceram.*, 1987, **7**(4), 200–204.
35. Amorós, J. L., Beltrán, V., Negre, F. and Escardino, A., Estudio de la compactación de soportes cerámicos (Bizcochos) de pavimento y revestimiento. II. Influencia de la presión y humedad de prensado. *Bol. Soc. Esp. Ceram. Vidr.*, 1983, **22**(1), 9–18.
36. Amorós, J. L., Escardino, A., Beltrán, V. and Enrique, J. E., Quality control in tile production. *Interceram*, 1984, **33**(2), 50–54.
37. Fahad, M. K., Stresses and failure in the diametral compression test. *J. Mater. Sci.*, 1996, **31**, 3723–3729.
39. Amorós, J. L., Sánchez, E., Cantavella, V., Jarque, J. C., Monzó, M., Timellini, G. and Leak, N., Effect of the drying cycle on dried tile mechanical strength. *Key Eng. Mater.*, 2002, **206–213**, 1663–1666.
40. Amorós, J. L., Sánchez, E., Cantavella, V. and Jarque, J. C., Evolution of mechanical strength of industrially dried ceramic tiles during storage. *J. Eur. Ceram. Soc.*, 2003, **23**, 1839–1845.
41. Davies, D. G. S., The statistical approach to engineering design in ceramics. *Proc. Br. Ceram. Soc.*, 1973, **22**, 429–452.
42. Quinn, G. D., Weibull strength scaling for standardized rectangular flexure specimens. *J. Am. Ceram. Soc.*, 2003, **86**(3), 508–510.
43. Swank, L. R., Caverly, J. C. and Allor, R. L., Experimental errors in modulus of rupture test fixtures. *Ceram. Eng. Sci. Proc.*, 1990, **11**(9–11), 1329–1345.

44. Amorós, J. L., Orts, M. J., Sanz, V. and Escardino, A., Prensado unidireccional de polvos cerámicos aglomerados por atomización. I. Mecanismo de compactación, Ciencia y Tecnología de los materiales cerámicos y vítreos. *Faenza Editrice Iberica*, 1990, 133–137.
45. Amorós, J. L., Orts, M. J., Monfort, E. and Escardino, A., Prensado unidireccional de polvos cerámicos aglomerados por atomización. II. Microestructura de la pieza en Crudo, Ciencia y Tecnología de los materiales cerámicos y vítreos. *Faenza Editrice Iberica*, 1990, 139–144.
46. Neergaard, L. J., Neergaard, D. A. and Neergaard, M. S., Effective volume of speciments in diametral compression. *J. Mater. Sci.*, 1997, **32**, 2529–2533.